RSC Advances

ROYAL SOCIETY OF CHEMISTRY

www.rsc.org/advances

Ag-doped MnO_x electrode with high specific capacitance of 825 F/g has been fabricated by cathodic deposition method for supercapacitor.

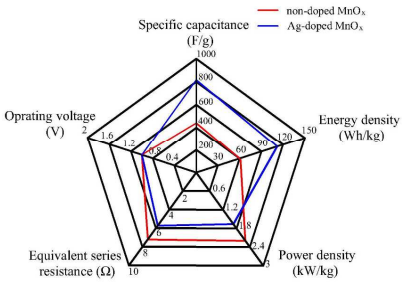

Ag-doped manganese oxide prepared by electrochemical deposition on carbon fiber for supercapacitors

Zifan Zeng[†], Ping Su[†], Jiliang Zhu[*], Xiaohong Zhu

Department of Materials Science, Sichuan University, 610064 Chengdu, China

Abstract

The Ag-doped manganese oxide was deposited on carbon fiber via cathodic reduction method, then the deposits were dehydrogenized and oxidated by heat treatment at 350 ℃ for 4 h. Scanning electron microscopy, X-ray diffraction and X-ray photoelectron spectroscopy were utilized to characterize the structure and state of the deposits. The results show that manganese oxide presents amorphous fibrous structure and is a mixture of tetravalent and trivalent. The cyclic voltammetry curves measured with three-electrode methods in 0.5 M Na_2SO_4 electrolyte reveal that the specific capacitance of manganese oxide without and with Ag is about 450 and 825 F/g at the scan rate of 5 mV/s, respectively. Hence, Ag doping improves the pseudo-capacitor behavior. The MnO_x-based supercapacitors fabricated with 0.5 M Na_2SO_4 as electrolyte are characterized by cyclic voltammetry and galvanostatic charge–discharge to investigate the electrochemical properties. In order to study the cycle life of the devices the galvanostatic charge-discharge process is cycled 3000 times and the specific capacitance almost keeps no change after 3000 cycles.

1. Introduction

[†] These authors contributed equally to this work. [*] Corresponding author. Tel.:+86 28 85432078; fax:+86 28 85432078. *Email address*: jlzhu167@scu.edu.cn (J. Zhu).

Supercapacitors, also known as electrochemical capacitors, are regarded as potential energy storage devices for hybrid electric vehicles, power sources and portable electric devices because of fast charging/discharging rate, high power density, good chemical stability and long cycle life compared to the lithium batteries.[1-5] On the basis of the different electrode materials, the electrodes of electrochemical capacitors are currently classified into carbon electrode, transition metal oxide, conducting polymer and hybrid composites.[4, 6, 10] In general, the electrochemical capacitors based on carbon as electrode store energy by physical process of electrostatic charge diffusion and accumulation at the interface of the electrode/electrolyte, named as electrical double-layer capacitors, whereas transition metal oxide and conducting polymer by chemical process highly reversible Faradaic electrochemical redox on surface of electrode, named as pseudo-capacitors.[6-10] So pseudo-capacitors possess higher energy density (of the order of hundreds of macro farads per square centimeter) than electrical double-layer capacitors (of the order of tens) in the same situation. Manganese oxide, one of electrode materials for pseudo-capacitors, has received extensive research in recent years.[3-6, 13, 14] As a most competitive candidate, MnO_2 has gained enormous attention on account of natural abundance, superior electrochemical performance, environment-friendly nature and low cost.[1, 11, 15-31, 40-42]

Many physical or chemical techniques have been used to prepare manganese oxide for electrode application in electrochemical capacitors, such as hydrothermal method, sol-gel method, electrostatic spray, sputtering, and electrochemical deposition.[16] Among of those methods, significant interest in electrochemical

deposition for manganese oxide film is generated because the process can be easily performed on conductive substrates of complex shape and preciously control of the film thickness is enable to be implemented by regulating the electrical charge delivered during electrolysis.[1] Usually, electrochemical deposition for preparing manganese oxide is segmented into anodic oxidation and cathodic reduction. Anodic oxidation manufactures manganese oxide film by the way that manganese ions loss electron on the surface of substrate to change from low valence to high valence.[1, 5, 12, 19, 20, 23-29] Amorphous $MnO_x \cdot nH_2O$ films prepared by anodic deposition has been reported in the literature.[25] The film manifests a good specific capacitance (about 320 $F\ g^{-1}$) at the potential scan rates of 5mV s^{-1}, high reversibility and high pulse charge/discharge properties.[25] However, anodic oxidation cannot be used for deposition of manganese oxide on metallic substrates due to the fact that the metallic substrates can absorb electron leading to an occurrence of dissolving in the solution.[18] This problem can be avoided by cathodic deposition because high valence of manganese transforms to low valence of manganese when the manganese ions absorb electron on the substrate surface.[15, 17, 18, 30-32, 43]

According to the mechanism of storage energy of pseudo-capacitors, the redox reaction of manganese generates on the electrodes and the electrolyte interface.[9, 10] Therefore, it is critical for the effective utilization of electrodes mass since charges transfer and diffuse during charge/discharge, which has been demonstrated by decrease of specific capacitance with the increase of the thickness of manganese oxide film. In addition, cations in the electrolyte and protons participate in the process of

charges transfer and diffusion.[1, 9, 33] From the above, the factors that influence electrochemical properties of manganese oxide film are believed to mainly include morphology, structure and conductivity of electrodes.[17] The manganese oxide prepared by anodic oxidation, which transforms from low valence to high valence, and manganese oxide prepared by cathodic reduction, for which the Mn ions direct vary from high valence to low valence during electrolysis, both present layered structure lying parallel to the electrode surface.[15, 24, 27] This makes it difficult for charge-compensating cations to conduct along a direction perpendicular to the electrodes surface.[1] A cathodic deposition of fibrous manganese oxide film performed in the solution containing Mn^{2+} ions, whose structure is nanofiber, enables this problem to be solved.[15] The deposition procedure shown in equation (1) produces $Mn(OH)_2$ deposit, then $Mn(OH)_2$ transforms MnO_x film by dehydrogenation and oxidation.

$$Mn^{2+} + 2H_2O + 2e^- \rightarrow Mn(OH)_2\downarrow + H_2\uparrow \qquad (1)$$

On the other hand, manganese oxide itself is a semiconductor and its low conductivity (10^{-5}~10^{-6} S cm^{-1}) also limits charges transfer, which results in the real value of specific capacitance lower than the theoretical value.[9, 17, 18, 34, 35] The composite electrodes mixing manganese oxide with highly conductive materials, such as metal nanoparticles,[18] carbon nanotubes,[34] conductive polymer[35] and graphene,[36] have been extensively researched to improve the electrical conductivity. In our present work, Ag-doped MnO_x with fibrous structural and good electrochemical performance was applied to the electrode for electrochemical capacitors via cathodic codeposition

in the solution containing Mn^{2+} ions and glucose.

2. Experimental section

2.1. Preparation of electrodes

The fibrous Ag-doped MnO_x film was synthesized on the carbon fiber by cathodic oxide method. The analytical-grade chemicals $AgNO_3$ and glucose (Chengdu Chron Chemicals Co., Ltd, China) were directly used without any further purification. $Mn(NO_3)_2$ (Chengdu Chron Chemicals Co., Ltd, China) is from the 50% mass concentration of solution. Firstly, $Mn(NO_3)_2$ was diluted into 200mL aqueous solution with 10 mM concentration. Then, 0.0341 g $AgNO_3$ and 2 g glucose were dissolved into the $Mn(NO_3)_2$ aqueous solution. The concentration of electrolyte is 10 mM $Mn(NO_3)_2$, 1 mM $AgNO_3$ and 1 g L^{-1} glucose. In order to study the influence of Ag doping, the same concentration electrolyte without $AgNO_3$ was prepared for comparison. Before electrochemical deposition, carbon fiber substrate (geometric area of 1×2 cm^2) needed to be cleaned with 2 % hydrochloric acid and 5 M potassium hydroxide in ultrasonic bath and dried at 80 ℃ for 1h.

Cathodic deposition was performed by applying a constant potential of -2.5 V in a common glass cell with the carbon fiber substrate as working electrode, a Ag/AgCl as reference electrode, and a platinum foil as counter electrode. It is necesseary to rigidly monitor charge delivered in order to control the active materials mass of 40 μg cm^{-2}. After electrodeposition, the electrodes were dried at 80 ℃ for 6h. Then glucose was resolved by heat treatment at 350 ℃ for 4h. The mass of active materials was decided by weighing the substrates before and after deposition experiments followed

by heat treatment at 350 ℃ for 4h.

2.2. Characterization

Fibrous nanostructure amorphous MnO_x films were characterized using scanning electron microscopy (SEM) (JSM-7500F, Japan), X-ray diffraction (XRD) (DX1000, China) with a CuKα radiation. The state of element was obtained by X-ray photoelectron spectroscopy (XPS) (XSAM 800, Kratos, UK). Characterization of electrochemical properties was perform by use of an electrochemical station (CHI 660E). The sample electrodes were measured with a cyclic voltammetry method in a three-electrodes system containing MnO_x film as working electrode, a Ag/AgCl as reference electrode, a platinum foil as counter electrode in 0.5 M Na_2SO_4 solution at a voltage window of 0 V to 0.8 V. In order to study the relation of MnO_x film electrodes and electrochemical capacitors, the capacitors based on MnO_x film were assembled with a separator and 0.5 M Na_2SO_4 solution as electrolyte. The electrochemical performances were characterized by cyclic voltammetry, galvanostatic and charge/discharge spectroscopy.

2.3. Calculation

Cyclic voltammetry can be applied for calculation of specific capacitance as follows: [10, 11, 18, 20]

$$C = \frac{\int_0^{0.8} Idu}{\Delta m \cdot U \cdot \nu} \qquad (2)$$

Where C is the specific capacitance of MnO_x, I is current of CV curve, Δm is the active materials mass of single electrode, U is the voltage of window 0.8V and ν is

the potential scanning rate.

It is feasible to obtain specific capacitance and the equivalent series resistance from galvanostatic charge/discharge curve. The specific capacitance equals current (I) multiplied by charge time (t), and subsequently divided by the Δm mass of active materials and potential window (U).[10, 11, 15, 17, 41, 44]

$$C = \frac{I \cdot t}{U \cdot \Delta m} \qquad (3)$$

3. Results and discussion

The mechanism of cathodically depositing manganese oxide from Mn^{2+} solution contains adsorption of ions and electrolysis of water working together, as shown in Fig. 1A. Cathode attracts positively charged Mn^{2+} ions to its surface because of electrostatic attraction in the electric field. The Mn^{2+} ions attracted on cathodic surface chemically react with OH^- generated from electrolysis of water around the cathode to produce $Mn(OH)_2$ and then deposit on the cathode with glucose as the binder. Whereafter, $Mn(OH)_2$ sediment is dehydrogenated and oxidized by drying and heat treatment and forms the MnO_x film.[15] Meanwhile, the process of silver deposition is also carried out, which was achieved by two different pathways. One of the pathways is that Ag^+ ions around the cathode directly gain electron to generate elemental silver. The other is transformation of sliver from sliver hydroxide with the same mechanism of manganese hydroxide deposition, that is, AgOH can easily decompose into argentous oxide and water, then the argentous oxide can turn to the elemental silver by heat treatment at 300 ℃. The temperature of heat treatment is

decided to be 350 ℃, judging from the facts that glucose entirely breaks down at 350 ℃ and MnO_x transforms into Mn_2O_3 at 400 ℃.[15]

Fig. 1B shows XRD pattern of the films co-deposited on the stainless steel substrate under the same condition as carbon fiber. The sample displays three strong peaks at 43.5°, 50.6° and 74.4° which are contributed from iron substrate. With the exception of three strong peaks, there is a broad weak peak at 37.1° corresponding to α-MnO_2, which reveals that the deposited films contain manganese oxide. This agrees with a number of manganese oxide films prepared by electrochemical deposition methods in the literatures.[15, 16] The weak peak intensity results from the poor crystalline and very thin thickness of manganese oxide films. The peaks related to silver are not found in the XRD pattern since silver does not crystallize and the content of silver is too small to be detected by X-ray diffraction.

The surface appearance of electrodes deposited by cathodic reduction from Mn^{2+} solution with sliver and without silver was investigated using scanning electron microscopy (Fig. 2). It shows that the carbon fiber surface after electrodeposition, regardless of doping Ag (Fig. 2C) and non-doping Ag (Fig. 2B), appears rougher than the surface without electrodeposition (Fig. 2A), impling that there are deposits produced on carbon fiber by plating. Under higher magnification, the morphology of pure MnO_x deposits displays a porous and fibrous 3D network (Fig. 2D). The pore size is about 40~80 nm and fiber length is about 100~400 nm. The nanostructure is profitable for ion transportation and effective utilization of manganese oxide, thereby resulting in the improvement of electrochemical properties.[15] However, doping sliver

reduces the length of fiber and the fiber interval (Fig. 2E), suggesting that sliver limits growth of MnO_x fiber. The length of fiber is measured about 80~200 nm and interval size is about 10~30 nm.

The chemical element state and component of electrodes obtained by cathodic deposition with sliver and without sliver were investigated by XPS (Fig. 3A). It shows that Mn 2p, Mn 3s and O 1s peaks are attributed to manganese oxide and the C 1s peak relates to substrate, which confirms it is accessible to cathodically deposit manganese oxide from Mn^{2+} ions. The presence of Ag 3d peak on the Ag-doped spectra is attributed from doping Ag in manganese oxide. Besides, the Si 2s and Si 2p corresponding to silicon dioxide (proved from O 1s peak later) appear at both Ag-doped and Ag non-doped spectroscopy. SiO_2 was impurity brought in during the process of preparing electrodes. Table 1 summarizes the position and component of Mn 2p, O 1s, C 1s and Ag 3d core level spectrum from XPS spectra. The positions of Mn 2p and O 1s peak with and without Ag is about 639.0 eV and 526.5 eV respectively, indicating that the oxidation state of manganese oxide almost does not change.[39, 44] The result is also confirmed by the same atomic ratio of Mn/O (about 1:2) before and after doping Ag. Quantitative calculation of sliver percentage composition based on atomic Ag/Mn ratio after exclusion of C shows doping amount of sliver is about 4.2 %. The Ag 3d core level spectra (Fig. 3B) can be used to investigate valance of sliver. The positions of Ag $3d_{5/2}$ and $3d_{3/2}$ peak located at 368.2 eV and 374.3 eV respectively are concordant with the positions of elemental silver peaks.[37] Thus it is believed that the elemental sliver has been doped into the MnO_x during

electrochemical deposition.

film	peak	Position (eV)	FWHM (eV)	Area (cps eV)	Atomic Conc %	Mass Conc %
non-doped	Mn 2p	639.05	3.050	81090.9	10.87	34.10
	O 1s	526.50	1.353	45055.0	20.94	13.19
	C 1s	281.40	0.752	50005.5	68.19	46.77
Ag-doped	Mn 2p	638.90	3.257	95658.3	13.30	37.77
	O 1s	526.60	1.526	55395.0	26.70	22.08
	C 1s	281.40	0.821	42016.3	59.42	36.90
	Ag 3d	364.65	1.184	9013.9	0.58	3.25

Table 1 All elemental data from XPS spectra of the films with non-doped and doped Ag.

Since MnO_x compound is composed of manganese and oxygen coalescing by covalent bond generated by blending unpaired electron of valence shell, the O 1s core level spectra (Fig. 3C) can be used to assess the valence and oxidation state of manganese for the electrodes.[9, 12, 19, 33] From the Fig. 3C, it is obvious that the O 1s peak is a mixed peak consisting of three peaks. The results from calculating the O 1s peak by Gaussian peak split are displayed at Table 2. It shows that the three peaks located at 529.6 eV, 531.3eV and 533.9eV are attributed to the Mn−O−Mn bond, Mn−OH bond and Si−O−Si bond, respectively. The Mn−OH bond represents MnOOH related to trivalent manganese. As MnOOH also contains the Mn−O−Mn bond, the Mn−O−Mn bond represents MnO_2 related to tetravalent manganese and MnOOH.[9, 19] The component of tetravalent manganese species is computed by subtracting the contribution of the Mn−OH bond from Mn−O−Mn bond. Hence, the contents of tetravalent and trivalent manganese from pure MnO_x is 23.3 % and 27.2 %, compared

to 16.5 % and 29.3 % for Ag-doped MnO_x. The oxidation state can be computed from the content of trivalent and tetravalent manganese according to

$$S_{ox} = \frac{4S_{te} + 3S_{tr}}{S_{te} + S_{tr}} \quad (4)$$

where S_{ox} is the oxidation state of manganese, S_{te} and S_{tr} respectively represent the component of tetravalent and trivalent manganese.[9] The MnO_x specimens deposited without silver and co-deposited with silver present similar oxidation state (3.5 and 3.4, respectively), demonstrate that doping Ag dose not obviously influence the oxidation state of the MnO_x deposited by cathodic reduction.

The multiplet splitting of Mn 3s peaks is also useful for studying oxidation state of manganese for Ag-doped and non-doped MnO_x. The Mn 3s peak separation of electrons in the core level with unpaired electrons in the valence band level is caused by the electron exchange interaction in the 3s-3d core level, which reveals that the energy separation of the Mn 3s peaks has a linear relation with the oxidation state of manganese.[9, 19] The Mn 3s peaks shown in Fig. 3D and table 2 indicate the energy separation of 5.1 eV without sliver and 5.2 eV with silver, respectively. According to the energy separation of 5.79, 5.50, 5.41 and 4.78 eV for reference samples of MnO, Mn_3O_4, Mn_2O_3 and MnO_2 ,[9, 33] 5.1 eV or 5.2 eV locates between 4.78 eV and 5.41 eV. Therefore, it is supposed that the MnO_x plated by cathodic reduction from Mn^{2+} ions consists of Mn_2O_3 and MnO_2. The components of tetravalent and trivalent manganese, estimated from the energy separation of Mn 3s peaks, are 49.2%, 51.8% for

non-doped MnO_x and 33.3%, 66.7% for Ag-doped MnO_x, respectively. In other words, the oxidation state of Mn is 3.5 and 3.3, respectively, for non-doped and Ag-doped MnO_x, which is similar to the result from O 1s peak.

film	Mn 3s (eV)			O 1s (eV)			oxidation state Mn 3s/O 1s
	Peak 1	Peak 2	ΔeV		BE (eV)	Area %	
non-doped	84.6	89.7	5.1	Mn-O-Mn	529.6	50.5	3.5/3.5
				Mn-OH	531.3	27.2	
				O-Si-O	533.9	22.3	
Ag-doped	84.4	89.6	5.2	Mn-O-Mn	529.7	45.8	3.3/3.4
				Mn-OH	531.2	29.3	
				O-Si-O	533.9	24.9	

Table 2 The data for Mn 3s and O 1s core level spectrum of the films with non-doped and doped Ag.

To gain more information about the oxidation state of manganese, Mn 2p core level spectrum is investigated in detail (Fig. 3E). It shows that the positions of Mn $2p_{3/2}$ and Mn $2p_{1/2}$ peaks locates at 642.1 eV and 653.7 eV respectively for the deposits with and without doping Ag, whereas the reference sample positions of Mn $2p_{3/2}$ and Mn $2p_{1/2}$ peaks for Mn(Ⅲ), Mn(Ⅳ) is 641.7 eV and 653.3 eV, 642.2 eV and 653.8 eV, respectively. So it is reasonable to assume that Mn $2p_{3/2}$ and Mn $2p_{1/2}$ peaks are mixed peaks composed by Mn(Ⅲ), Mn(Ⅳ).[12] The results shown in Table 3 reveal that doping Ag in MnO_x by cathodic reduction almost does not change the oxidation state of manganese. The conclusion is supported by Mn 3s and O1s peaks.

The cyclic voltammetry curves for studying the electrochemical performance of MnO_x non-containing and containing silver deposited on carbon fiber by cathodic reduction were tested using three-electrode method with voltage scan rate of 100 mV s^{-1}, 50 mV s^{-1}, 20 mV s^{-1}, 10 mV s^{-1} and 5 mV s^{-1} in 0.5M Na_2SO_4 solution, as shown in Fig. 4A and B, respectively. They reveal that MnO_x electrodes non-doped and doped with Ag present typical electrochemical capacitance behavior. When the scanning speed is lower than 50 mV s^{-1}, a peak representing anodic oxidation from trivalent manganese to tetravalence appears at CV curves around 2.7 V.[38] It is the Ag-induced increase in the conductivity of active material that makes MnO_x more effectively to participate in redox process leading to strengthened pseudo-capacitance behavior. However, there is no redox peak in the CV curve without doping, indicating that the MnO_x doped with Ag has better pseudo-capacitance behavior.

film	Mn $2p_{3/2}$		Mn $2p_{1/2}$		ΔBE (eV) Mn-O
	tetravalent %	trivalent %	tetravalent %	trivalent %	
non-doped	95.1	4.9	92.2	7.8	112.5
Ag-doped	88.1	11.9	88.5	11.5	112.4

Table 3 The component of Mn^{4+} and Mn^{3+} computed from Mn 2p core level.

According to CV curve, the specific capacitance is calculated by equation (2) at different scan rates and the result is displayed in Fig. 4C. As the scan rate decreases from 100 mV s^{-1} to 5 mV s^{-1}, the specific capacitance of MnO_x both doped and non-doped gradually increase. Above the scan rate of 50 mV s^{-1}, the specific capacitance of MnO_x containing Ag is lower than MnO_x non-containing Ag. The phenomena can be explained with SEM images of MnO_x with and without silver.

Capacitance behavior is mainly influenced by diffusion process of ions and proton at high scan rate. The SEM images have confirmed that the morphology of MnO_x doped with Ag is more compact than non-doped MnO_x. The compact morphology results in limitation of ions and proton diffusion. Thus, MnO_x without Ag appears higher specific capacitance at high scan rate. However, charge transfer process determines the electrochemical performance of capacitors at low scan rate. Charge transfer process is related with active materials conductivity. The co-deposition of MnO_x and silver improves conductivity of manganese oxide and thus gives rise to higher specific capacitance at low scan rate. In addition, the specific capacitance of MnO_x without Ag is 450 F g^{-1} at scan rate of 5 mV s^{-1}, which is approximately the specific capacitance of ~ 400 F g-1 reported in literature.[15] Doping Ag improves specific capacitance to 825 F g^{-1} at the scan rate of 5 mV s^{-1}. The value is even higher than the specific capacitance of 770 F g^{-1} synthesized by cathodic co-deposition of manganese oxide and silver from Mn^{7+} electrolyte reported by Yaohui Wang et al.[18] The consequence is caused by the microstructure of electrode. The Ag-doped manganese oxide obtained from Mn^{7+} electrolyte presents porous structure, yet the microstructure of MnO_x with Ag deposited from Mn^{2+} solution is nanofibrous. The fibrous structure enables manganese oxide to be more effectively utilized to increase the specific capacitance.[1, 16]

In order to investigate electrochemical performance of as-prepared Ag-doped MnO_x used as supercapacitor electrode, two pieces of the carbon fiber with Ag-dopoed MnO_x was assembled into devices with 0.5 M Na_2SO_4 as electrolyte. The

devices were characterized by different methods including cyclic voltammetry, galvanostatic charge–discharge. The data of cyclic voltammetry at the scan rate of 5 mV s^{-1} (Fig. 5A) shows that the MnO_x doped with Ag displays better capacitance behavior (including larger faradic current and area of cyclic voltammetry curve) in comparison with non-doped MnO_x. The specific capacitance of manganese oxide with and without Ag computed by equation (2) from CV curve are about 810 F g^{-1} and 430 F g^{-1} at the scan rate of 5 mV s^{-1}, respectively. The values are similar to the specific capacitance tested by three-electrode way, revealing that the electrode keep good uniformity.

The galvanostatic charge-discharge properties were characterized by chronopotentiometry with different current density of 10 A g^{-1}, 5 A g^{-1}, 4 A g^{-1}, 3 A g^{-1}, 2 A g^{-1}, 1 A g^{-1} and 0.5 A g^{-1}, shown in Fig. 5B (non-dope) and Fig. 5C (Ag-doped). From the constant current charge-discharge curves, it is not difficult to conclude that charging or discharging duration time of the MnO_x containing Ag is longer than the MnO_x non-containing Ag, revealing the MnO_x containing Ag has larger capacitance. The specific capacities of manganese oxide with and without Ag ccalculated by equation (3) are 815 F g^{-1} and 440 F g^{-1} at the constant current density of 0.5 A g^{-1}. Moreover, a larger voltage drop of MnO_x with Ag, contributed to the equivalent series resistance (ESR), can be observed at the same current comparing with non-doped MnO_x. It confirms that MnO_x conductivity is improved by doping silver, a good electrical conductivity.

Manifold cycles were used to characterize the cyclic stability, thus determining

the cycle life of devices. As shown in Fig 5D, the galvanostatic charge-discharge processes of MnO_x with Ag are performed 3000 cycles at the current density of 3 A g^{-1}. The increase in specific capacitance in initial cycles is observed, which attributed to the electrochemical oxidation of MnO_x.[15] After 200 cycles, the device reaches stabilization and remains specific capacitance unchanged until to 3000 cycles. So, it is considered that the devices have long cyclic life. The increase in specific capacitance at initial 20 cycles, as shown in Fig. 5D, is contributed from that as-prepared manganese is the mixture of tetravalent and trivalent manganese, which has been demonstrated by XPS.

Electrochemical impedance spectroscopy (EIS) was performed to further investigate the Ag-doped MnO_x capacitive behavior associated with resistance of the electrode and the corresponding Nyquist plots are displayed in Fig. 6. The electrochemical impedance test was carried out at 5 mV amplitude (vs.Ag/AgCl) with a frequency range of 0.01 Hz to 1000000 Hz. Nyquist plots are composed of a semicircle in the high frequency region and a straight line in the low frequency region. The intercept of real axis and the Nyquist plots indicate the inner resistance for capacitor which is a combinational resistance of electrolyte resistance, intrinsic resistance of substrate and contact resistance at the active materials/current collector interface. Obviously, Ag-doped MnO_x had a relatively lower contact resistance (about 5.7 Ω) than non-doped MnO_x (about 7.5 Ω), revealing the active materials MnO_x and the conductive Ag could contact with each other closely, which could increase the electrical conductivity of electrode. The slope of the curves in the low frequency

region showed the Warburh impedance, which represented the electrolyte diffusion in the porous electrode and proton diffusion in the host material. As shown in Fig. 6, Ag-doped MnO_x had also a relatively steeper slope of the straight line especially in the low frequency region demonstrating Ag-doped MnO_x facilitated smoother charges transfer and ion diffusion.

A radar plot was employed to show the overall performance of as fabricated assembled devices with MnO_x electrodes (with/without Ag doping) as shown in Fig. 7. Red and blue curves represented the supercapacitor with non-doped MnO_x electrode and Ag-doped MnO_x electrode, respectively. They were generated by connecting the electrochemical performance data points. In general, a larger area encompassed within a radar plot indicates better overall performance.[10] The power density (1.66 kw kg^{-1} for Ag-doped MnO_x and 2.20 kw kg^{-1} for non-doped MnO_x), energy density (113 Wh kg^{-1} for Ag-doped MnO_x and 61 Wh kg^{-1} for non-doped MnO_x) and specific capacitance were calculated from charge/discharge curves at a scan rate of 0.5 A g^{-1}. The supercapacitor with non-doped MnO_x electrode owned a higher power density on account of that it has a looser structure which facilitates the ion and proton diffusion. However, the supercapacitor with Ag-doped MnO_x electrode owned higher specific capacitance, higher energy density and lower equivalent series resistance.

4. Conclusion

Cathodic co-deposition has been utilized for the fabrication of Ag-doped fibrous MnO_x electrode on carbon fiber. The XRD pattern indicates that the structure of MnO_x is α-MnO_2. From the SEM images, the MnO_x presents fibrous nanostructure and

doping Ag makes as-prepared MnO_x rougher. The XPS data indicate that the silver of about 4.2 % doping amount appears elemental and rarely influences the oxidation state of manganese oxide compared to MnO_x without Ag. The manganese dose not only contain tetravalent, but is a mixture of tetravalent and trivalent manganese. It needs many times charge-discharge cycles to achieve all effective manganese transition between trivalent and tetravalent. The CV curves of samples measured with three-electrode methods in 0.5 M Na_2SO_4 electrolyte show that doping Ag improves the electrochemical performance and the specific capacitance calculated is about 825 F g^{-1} at the scan rate of 5mV s^{-1}. The MnO_x assembled supercapacitor devices with 0.5 M Na_2SO_4 as electrolyte are characterized by cyclic voltammetry and galvanostatic charge-discharge. The results reveal that the devices keep good uniformity and the ESR is decreased by doping Ag in MnO_x. According to manifold cycles, the specific capacitance almost keeps no change after 3000 cycles. Thus, the Ag-doped MnO_x fabricated by this method can be used for applications in electrochemical capacitors.

Acknowledgements

This work was supported by the National Science Foundation of China (51472172, 11075110). The authors acknowledge the helps of Ms Hui Wang of Analytical and Testing Center of Sichuan University for SEM analysis.

References

1. M. Nakayama, T. Kanaya, R. Inoue, Electrochem. Commun. 2007,**9** , 1154.

2. S. S. Shinde, G. S. Gunda, D. P. Dubalb, S. B. Jamburea, C. D. Lokhande,

Electrochim. Acta. 2014,**119**, 1.

3. Y. W. Zhu, S. Murali, M. D. Stoller, K. J. Ganesh, W. Cai, P. J. Ferreira, A. Pirkle, R. M. Wallace, K. A. Cychosz, M. Thommes, D. Su E. A. Stach, R. S. Ruoff, Science 2011, **332**, 1537.

4. Y. Zhai, Y. Dou , D. Zhao , P. F. Fulvio, R. T. Mayes, S. Dai, Adv. Mater. 2011, **23,** 4828.

5. J. K. Chang, S. H. Hsub, W. T. Tsai, I. W. Sun, J. Power. Sources 2008, **177**, 676.

6. M. Yu, T. Zhai, X. Lu, X. Chen, S. Xie, W. Li, C. Liang, W. Zhao, L. Zhang, Y. Tong, J. Power. Sources 2013, **239**, 64.

7. C. Merlet, B. Rotenberg, P. A. Madden, P. L. Taberna, P. Simon, Y. Gogotsi, M. Salanne, Nat. Mater. 2012, **11**, 306.

8. H. Erny, Z. Abidin, A. A. Hamzah, B. Y. Majlis, J. Yunas, N. A.l Hamid, U. Abidin, Microelectron. Eng. 2013, **111,** 3748.

9. M. Toupin, T. Brousse, D. Belanger, Chem. Mater. 2004, **16,** 3184.

10. G. P, Xiong, C. Z. Meng, R. G. Reifenberger, Pedro P. Irazoqui, T. S. Fisher, Electroanalysis 2014 ,**26**, 30.

11. G. P. Xiong, K.P.S.S. Hembram, R.G. Reifenberger, T S. Fisher, J. Power Sources, 2013, **227,** 25412. C. C. Hu, C. C. Wang, J. Electronchem. Sco. 2003, **150**, 1079.

13. S. L. Candelaria, B. B. Garcia, D. Liu, G. Cao, J. Mater. Chem. 2012, **22**, 9984.

14. X. Lu, X. Huang, S. Xie, T. Zhai, C. Wang, P. Zhang, M. Yu, W. Li, C. Liangb, Y, Tong, J. Mater. Chem. 2012, **22**, 13357.

15. N. Nagarajan, M. Cheong, I. Zhitomirsky, Mater. Chem. Phys. 2007,**103**, 47.

16. D. L. Yan, Z. Guo, G. Zhu, H. Yang, R. Wei, H. Xu, A. Yu, Mater. Lett. 2012, **82**, 156.

17. J. Wei, N. Nagarajan, I. Zhitomirsky, J. Mater. Process. Technol. 2007, **186**, 356.

18. Y. Wang, I. Zhitomirsky, Mater. Lett. 2011, **65**, 1759.

19. M. Chiganez, M. Ishikawa, J. Electronchem. Sco. 2000, **147**, 2246.

20. S. C. Pang,a, M. A. Anderson, T. W. Chapman, J. Electronchem. Sco. 2000, **147**, 444.

21. M. Toupin, T. Brousse, D.l B.´langer, Chem. Mater. 2002, **14**, 3946.

22. W. Zhang, Z. X. Feng, L. X. Ze, J. N. Er, J. Porous Mater. 2010, **17**, 253.

23. M. Nakayama, S. Konishi, A. Tanaka, K. Ogura, Chem. Lett. 2004, **33**, 670.

24. M. Nakayama, S. Konishi, H. Tagashira, K. Ogura, Langmuir 2005, **21**, 354.

25. C. C. Hu, T. W. Tsou, Electrochem. Commun. 2002, **4**, 105.

26. C. C. Hu, T. W. Tsou, J. Power. Sources. 2003, **115**, 179.

27. P. Y. Chuang, C. C. Hu, Mater. Chem. Phys. 2005, **92**, 138.

28. S. Rodrigues, N. Munichandraiah, A. K. Shukla, J. Appl. Electrochem. 1998, **28**,1235.

29. Y. S. Chen, C. C. Hu, Y.T. Wu, J. Solid. State. Eletrochem. 2004, **8**, 467.

30. M. A. Cheney, S. W. Joo, A Banerjee, B. K. Min, J. Colloid Interface Sci. 2012, **379**, 141.

31. N. Nagarajan, H. Humadi, I. Zhitomirsky, Electrochim. Acta. 2006, **51**,3039.

32. T. Yousefi, R. Davarkhah, A. N. Golikand, M. H. Mashhadizadeh, Mater. Sci.

Semicond. Process. 2013, **16**, 868.

33. M. Chigane, M. Ishikawa, M. Izaki, J. Electronchem. Soc. 2001, **148**, D961.

34. H. Wang, C. Peng, F. Peng, H. Yu, J. Yang, Mater. Sci. Eng. B 2001, **176**, 1073.

35. W. Yao, H. Zhou, Yun Lu, J. Power. Sources 2013, **241**, 359.

36. C. J. Jafta, F. Nkosia, L. l. Rouxa, M. K. Mathea, M. Kebedea, K. Makgopac, Y. Songd, D. Tongd, M. Oyamae, N. Manyalab, S. Chend, K. I. Ozoemenaa, Electrochim. Acta. 2013, **110**, 228.

37. X. Wang, X. Houa, W. Luanb, D. Li, K. Yao, Appl. Surf. Sci. 2012, **258**, 8241.

38. J. W. Long, A. L. Young, D. R. Rolison, J. Electronchem. Soc. 2003, **150**,A1161.

39. Rahim Abdur,Kyungbae Kim, Jae-Hun Kim, Jaegab Lee, Electrochim. Acta. 2014, **11**, 187

40. S. Hassan, M. Suzuki, A. El-Moneim, J. Power. Sources. 2014, **246**, 68

41. N. Boukmouche, N. Azzouz, L. Bouchama, A. Daltin, J. Chopart, Y. Bouznit, Mater. Sci. Semicond. Process. 2014, **27**, 233

42. C. Liu, Z. Xie, W. P. Wang, Z. C. Li, Z. J. Zhang, Electrochem. Commun. 2014, **44**, 23

43. H. Sorkhabi, E. Asghari, P. Badakhshan, Curr. Appl. Phys. 2014, **14**, 187

44. N. Li, J. Y. Wang, Z. Q. Liu, Y. P. Guo, D. Y. Wang, Y. Z. Su, RSC Adv. 2014, **4**, 17274

Figure captions

Figure 1 Synthesis and structural characterizations of the MnO_x electrode. (***A***) Schematic illustration of the deposition process of $Mn(OH)_2$ deposits by cathodic reduction. (***B***) XRD pattern of Ag-doped MnO_x co-deposited on the stainless steel substrate.

Figure 2 Morphology characterizations of the MnO_x non-doped and doped with Ag on the carbon fiber by scanning electron microscopy (SEM). (***A***) SEM image of carbon fiber. (***B***) and (***C***) SEM images of the MnO_x non-doped and doped with Ag on the carbon fiber, respectively. (***D***) and (***E***) SEM images on higher magnification of the MnO_x without and with Ag on the carbon fiber, respectively.

Figure 3 The characterization of chemical element state and component of electrodes obtained by cathodically depositing with sliver and without sliver. (***A***) XPS investigation for the MnO_x without and with Ag. (***B***) The Ag 3d core level spectra of Ag-doped MnO_x electrode. (***C***) O 1s core level spectra for survey of the oxidation state of manganese. (***D***) and (E) Mn 3s core level spectra and Mn 2p core level spectra for survey of the oxidation state of manganese, respectively.

Figure 4 The investigation for electrochemical properties of non-doped and Ag-doped manganese oxide electrode with three-electrode method in 0.5 M Na_2SO_4 electrolyte. (***A***) and (***B***) Cyclic voltammetry curve of MnO_x electrode non-containing and containing Ag at the scan rate of 100 mV/s, 50 mV/s, 20

mV/s, 10 mV/s, 5 mV/s. (***C***) Effect of the voltage scan rate on the specific capacitance of MnO_x electrode.

Figure 5 The characterization for electrochemical properties of the devices with manganese oxide as electrode in 0.5M Na_2SO_4 electrolyte. (***A***) Cyclic voltammetry curve at the scan rate of 5 mV/S. (***B***) and (***C***) charge/discharge curve at the constant current density of 10 A/g, 5 A/g, 4 A/g, 3 A/g, 2 A/g, 1 A/g, 0.5 A/g. ***(D***) The devices stability survey using the variation of the specific capacitance as a function of the number of cycles.

Figure. 6 The Electrochemical Impedance Spectroscopy measurement of non-doped MnO_x and Ag-doped MnO_x

Figure. 7 A radar plot summarizing and comparing the performance of assembled devices with MnO_x electrodes (with/without Ag doping)

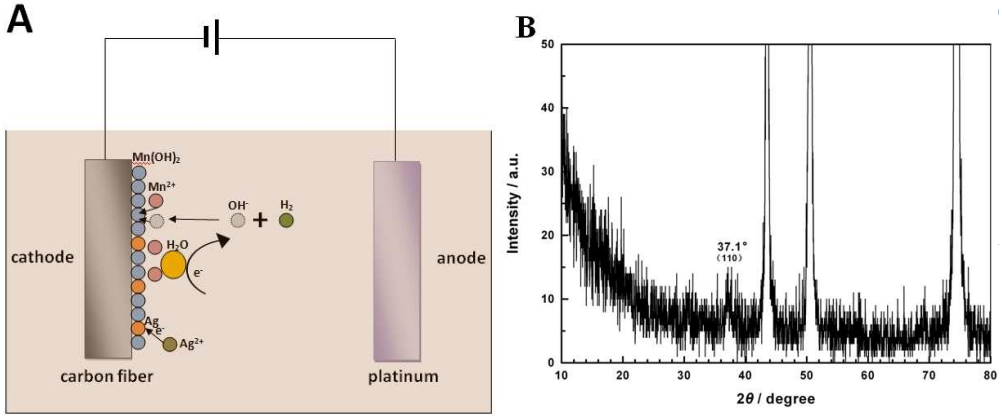

Figure 1

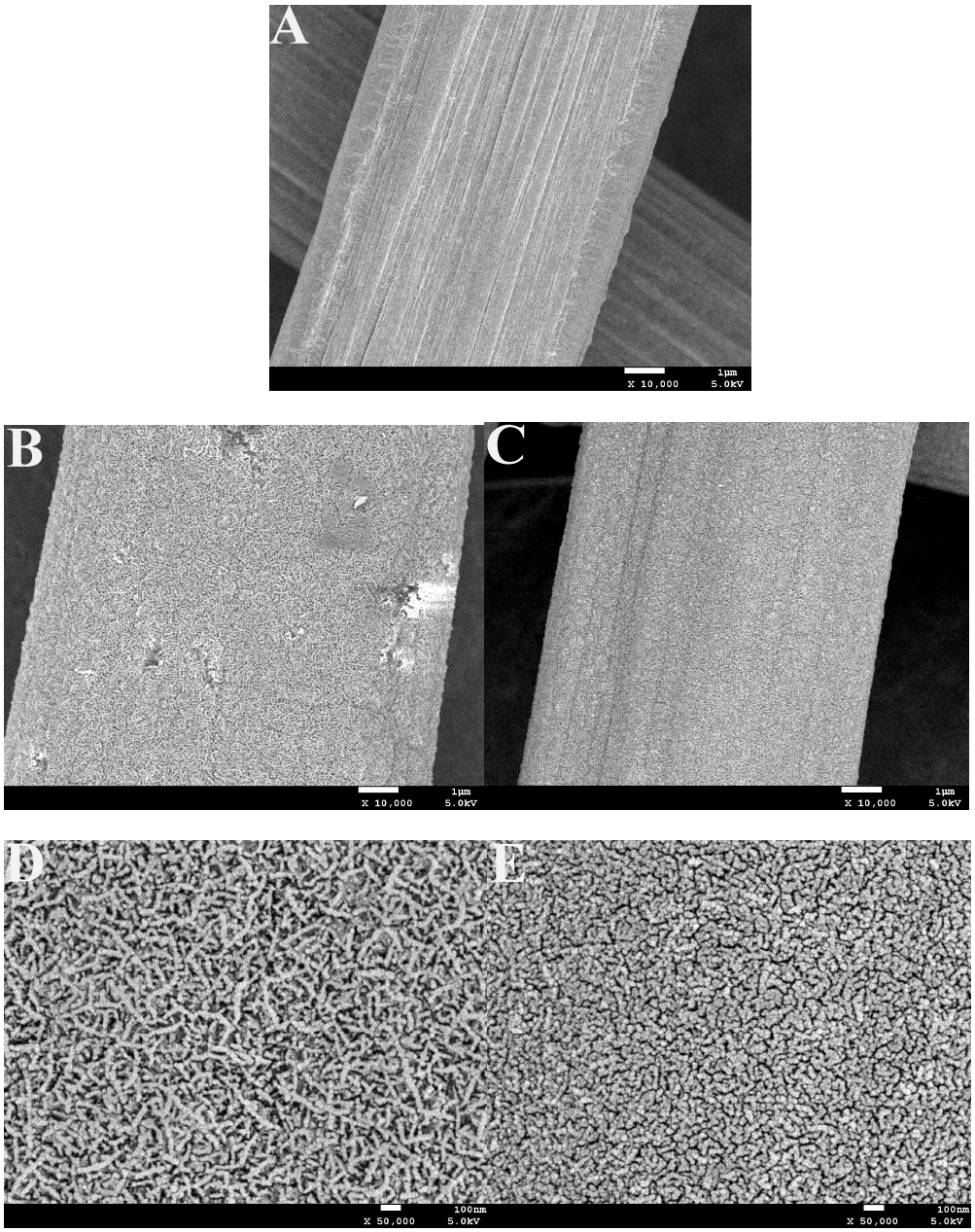

Figure 2

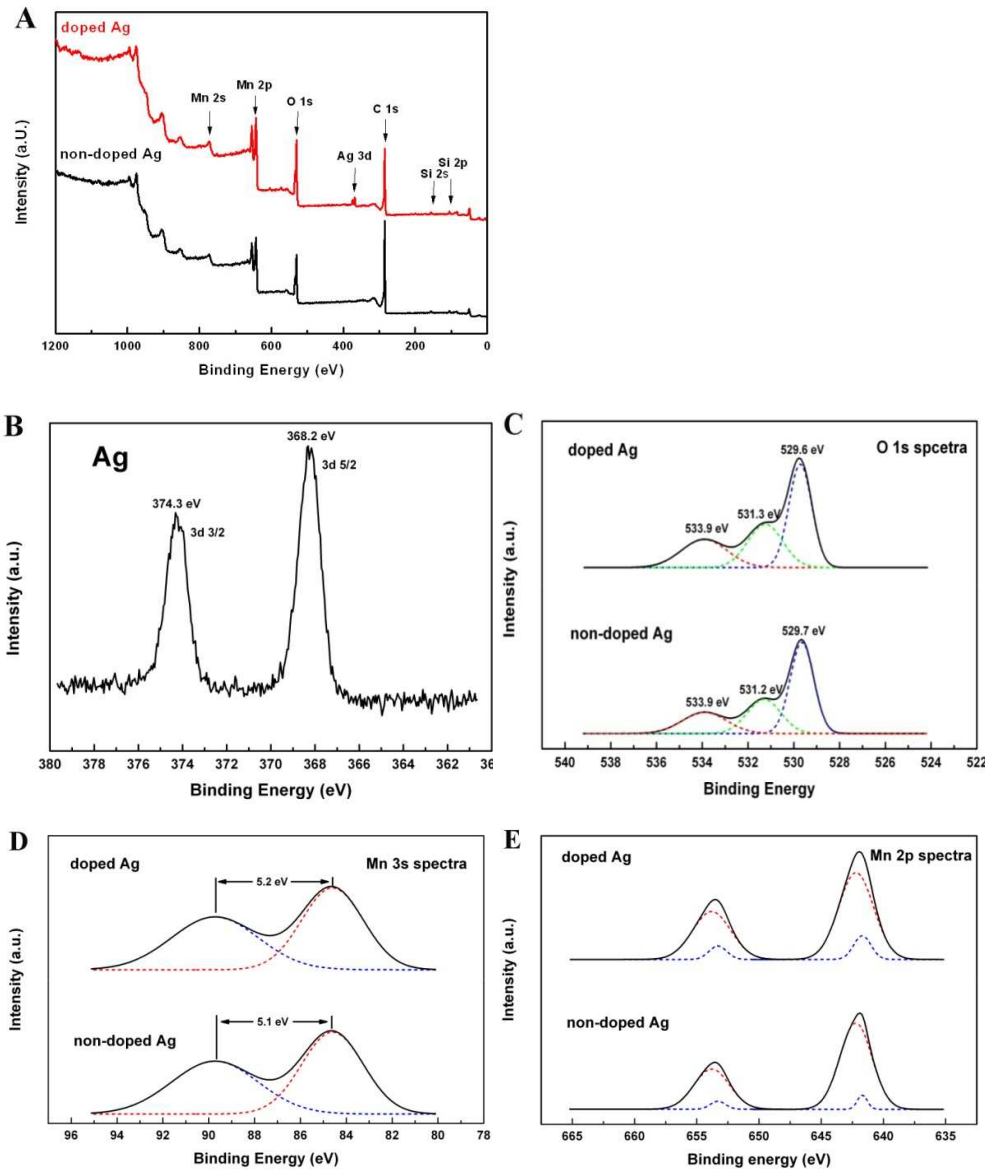

Figure 3

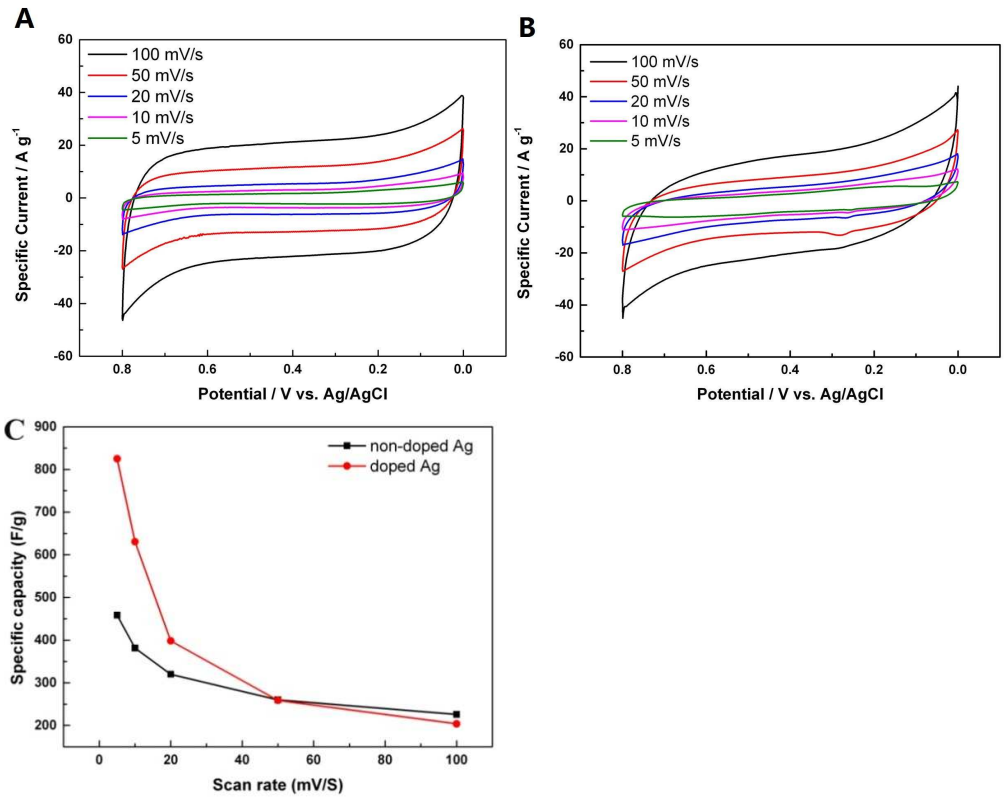

Figure 4

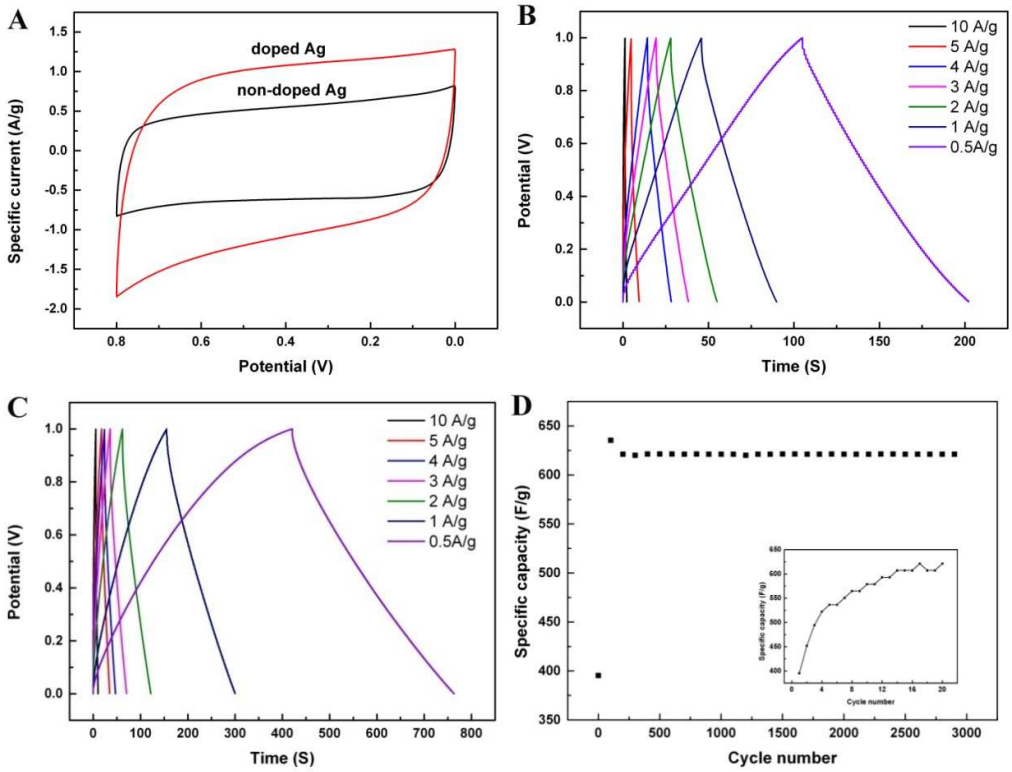

Figure 5

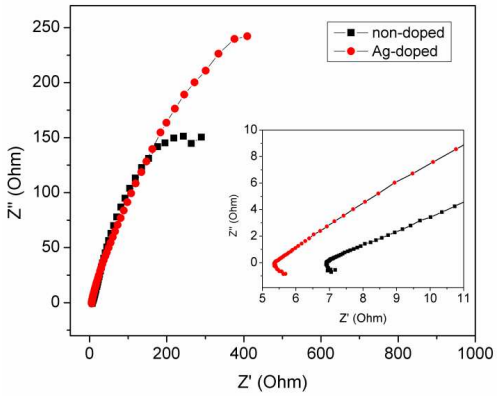

Figure. 6

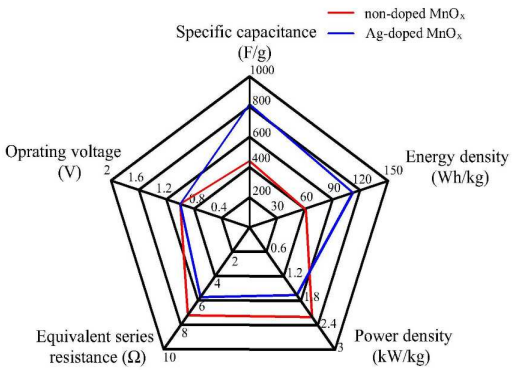

Figure. 7